Analysis of The Effect of Atmosphere-Ocean Interaction on Winter Rainfall in Iran

Atefe Ebrahimi
University of Isfahan
Dariush Rahimi (d.rahimi@geo.ui.ac.ir)
University of Isfahan
Daria Gushchina
Moscow State University (MSU)

Research Article

Keywords: Iran, Precipitation, Cold season, Correlation, SST, SLP

Posted Date: October 27th, 2022

DOI: https://doi.org/10.21203/rs.3.rs-2181555/v1

Additional Declarations: No competing interests reported.

Version of Record: A version of this preprint was published at Environmental Earth Sciences on April 5th, 2023. See the published version at https://doi.org/10.1007/s12665-023-10858-7.

Abstract

Decades of drought and heavy rainfall are the most important climatic hazards in Iran. Anomalies and concentration of winter rainfall are effective in the challenge and water shortage. Iran's rainfall is strongly influenced by teleconnection. So that changes in SLP[1],SST[2] and changes in the level of 500 hPa have an effective role in the temporal distribution and volume of rainfall. The effect of three factors of sea level pressure, 2.5°*2.5° were evaluated from 1984 to 2018.The results indicated that decreased pressure on the Red Sea (Sudan Low) and the Pacific Ocean and increased pressure on the Atlantic and Indian oceans increase Iran's winter precipitation. In 500hpa, the results indicated that increased winter precipitation in Iran is associated with an increase in altitude of 500hPa on the Baltic Sea and the Indian Ocean and a decrease in altitude of 500hPa on the Caspian Sea, the Mediterranean Sea, the Arabian Sea and the Red Sea. In SST, the results indicated that the linkage between SST and precipitation of Iran is positive in regions such as the Arabian and Red sea, Madagascar, and north Atlantic Ocean. Therefore, any change in sea level pressure, 500hPa level and sea surface temperature leads to positive and negative anomalies on Iran's rainfall. Therefore, global warming, which leads to changes in SLP, atmospheric thickness (1000-500) and SST, has a greater impact on Iran's rainfall and leads to challenges in water resources and climate risks.

[1] -Sea level pressure

[2] -Sea surface temperature

1. Introduction

In arid and semi-arid climates such as Iran, the temporal concentration of rainfall in limited months reduces the resilience of ecosystems to rainfall anomalies. In Iran, more than 50% of the annual rainfall occurs in winter. Therefore, the decrease in rainfall in each month of this season leads to moderate and severe droughts. Therefore, with the occurrence of drought and depletion of water resources, natural, economic and social challenges increase.

Seasonal rainfall analysis in Iran indicated that the decrease in rainfall in the winter months is effective in the occurrence of droughts (December and January 2015, January 2009, February and March 2008). Synoptic analysis of these droughts has indicated the effect of changes in SST, SLP, 500hPa and the existence of blocking systems.

The changes of SST, SLP,500hpa and Blocking system are related to the interaction of the ocean and atmosphere plays a significant role in forming the climate and its variations. One of the most important issues that affect these connections is the amount of precipitation and consequently the management of water resources.

Effectual management of water resources is important due to the population growth and increasing problems of access to fresh water in arid and semiarid areas like Iran (Meidani et al.,2014). In Iran, changes in precipitation caused by synoptic system (polar front, polar front jet stream, westerlies and etc..) and geographical factors (marine, continental, latitude, and elevation (height, lee slope and windward slope) (Barth & Steinkohl ,2004; Raziei et al.,2013; Sabziparvar et al.,2015).The synoptic patterns affecting Iran's rainfall also indicated that high pressure of Siberian and deep trough at the east of Mediterranean Sea and red sea, low pressure in Black sea and Monsoon are very important (Rasouli et al.,2012; Fatemi at al.,2015,Delju et al.,2013,Ahmadi et al,2019).

The results of studies indicated that the atmosphere and the ocean have an interaction. Sea surface temperature, sea level pressure, 500hpa and ocean currents are effective in spatial patterns and fluctuations of precipitation (Barnston and Livezey, 1987; Brown and Comrie, 2002; Saji et al., 2005; Roy, 2006; Gushchina & Dewitte, 2011; Barandiaran & Wang, 2014; Lee et al.,2016; Ptak et al., 2018, Rezaebanafsheh et al., 2011; Lu et al., 2016, Trenberth et al., 2005; van der Ent et al., 2013, Wibig, 1999; Xoplaki et al., 2000; Türkes et al., 2002). For example, These effects Iranian on rainfall by teleconnection patterns (i.e. ENSO, NAO, SCAND, IOD and etc.) with Iran’s hydrological cycle (Nazemosadat & Ghasemi, 2004; Motamedi et al., 2007; Dezfuli et al., 2010; -Azmoodehfar and Azarmsa, 2013; Farajzadeh et al., 2014).

Droughts (2018 – 2008) and heavy rains in 2019 in Iran indicate changes in precipitation in the cold season (DJF). Due to the effect of teleconnection on Iran's climate, analysis of the interaction atmosphere and ocean and the identification of spatial patterns of sea surface temperature, sea level pressure and the level of 500 hPa have an effect on these precipitation anomalies.

In this study, we try to investigate the effect of SST, SLP and 500 hPa on winter (DJF) rainfall in Iran. In addition, to determine in which parts of the world these changes are related to Iranian rainfall.

2. Data And Methods

2.1. Case study

Iran is situated in the southwest of Asia, between 25˚3´ N to 39˚47´N and 44˚5´E to 63˚18´E. Iran’s total area is approximately 1,648,195 km2. The climate of Iran is considered arid and semi-arid (Javari, 2016). This country has a diverse climatic condition across provinces with significant spatial differences in precipitation amount. The annual precipitation varies from about 1800 mm over the western Caspian Sea coast and western highlands to less than 50 mm over the uninhabitable eastern deserts. The precipitation regime in Iran is characterized by large variability in a wide range of timescales: from daily up to inter annual. Severe droughts are typical for the summer season while the highest rainfall occurs in winter (Nazemosadat et al., 2006; Darand & Daneshvar, 2014).

2.2. Data

Monthly mean SLP, SST and 500 hPa level of global gridded data with 2.5°*2.5° resolution were obtained from the NCEP/NCAR Reanalysis [3] (Kalnay et al.,1996). The monthly precipitation data derives from the Global Precipitation Analysis Products (GPCC) full data reanalysis V7.0 (Schneider et al., 2008) in period 1984–2018.The anomalies are calculated by removing the seasonal cycle averaged over the 35 years' period. The data for December, January, and February (DJF) were used.

2.3. Methods

The methodology used in this paper is divided into four main steps. First of all, we zoning precipitation in Iran using correlation. Then to determine the physical boundaries of precipitation regions, we used the kriging method. In third steps Pearson correlation was used to specified the places with high correlation with winter precipitation of Iran. Finally, multiple linear regression applied to find the best regression equation. To determine the effective areas in this study, the following conditions are considered: the correlation is more than 0.3, R^2 more than 0.55, the low difference between the R^2 and the R^2-adj, the P-value is less than 0.05, and the correlation between the calculated anomaly of precipitation and the observed data is greater than 0.7.

Pearson Correlation

Correlation in the vast meaning is a measure of an association between variables. In correlated data, a variable is correlated with another variable, either in the positive correlation or in the opposite (negative correlation) direction. correlation coefficients are scaled a range from − 1 to + 1, where 0 indicates that there is no linear or monotonic association (Schober etal.,2018). Pearson's coefficient of correlation was found by Bravais in 1846, but Karl Pearson was the first to explain, in 1896, the standard technique of its calculation. Pearson's correlation coefficient is a measure of the strength of the linear relevance between two variables (Hauke etal.,2011). Pearson correlation equation can be written as below

$$r = \frac{N\sum xy - (\sum x)(\sum y)}{\sqrt{\{N\sum x^2 - (\sum x)2\}\{N\sum y^2 - (\sum y)2\}}}$$

1

Where *N* = Number of pairs of values, $\sum x$= Sum of the *x* values, $\sum y$=Sum of the *y* values (Obilor etal., 2018).

Kriging Method

In geo-statistics, kriging or Gaussian process regression is a method of interpolation for which the interpolated values are modeled by a Gaussian process governed by prior covariance. Under suitable molds on the priors, kriging gives the best linear unbiased forecast of the intermediate values (Lichtenstern, 2013). Kriging Function is (Equ.2)

$$Z^* = \sum_{i=1}^{n} W_i\, Z(x_i)$$

2

Where: Z^* is Estimated spatial variable, $z(x_i)$ is observed spatial variable w_i is the weight of the variable statistic is the amount of observation.

Multiple Linear Regression

Regression analysis is a statistical method for estimating the relationship between a dependent and independent variable. The regression model with a dependent variable and a more independent variable is called multilinear regression. In multivariate regression analysis is formulated as

$$y = \beta_0 + \beta_1 x_1 + \ldots + \beta_n x_n + \varepsilon$$

3

Where y is dependent variable, x_i is independent variable, β_i as parameter and ε is error (Uyanik and Güler,2013).

According to the topography and changes in spatial precipitation, the kriging method was divided into eleven precipitation zones in the cell size of $2.5^{\circ}*2.5^{\circ}$ (Map No. 1 and Table No. 1). The correlation between precipitation at each grid point (26 green point in Fig. 1) and all adjacent grid points is calculated. The pixels correlated with a coefficient higher than 0.7 were merged in one precipitation area. Finally, the following 11 regions were detected for Iran (White frame in Fig. 1). Then used kriging to determine the physical boundaries of precipitation zones. zones 1,2,5, and 9 containing one grid point, zones number 4,8, and 11 containing two grid points, zone 7 covering three grid points, zones 3 and 6 containing four grid points, and lastly the largest zone, number 10 being combining five grid points.

Zone 1 corresponds to the valley of the Aras River, it is characterized by annual rainfall of 250 mm up 500 mm. Zone 2 is located in the northwest of Iran, it is characterized by relatively high precipitation amount (about 400 mm yearly). Zone number 3 is the most extensive, this area starts from northwest with annual rainfall of 950 mm and extends to the south of Iran with annual rainfall of 250 mm. There are, of course, some regions in the area with a rainfall of more than 1000 mm yearly. Fourth zone is located in the western Alborz and south of coast Caspian Sea. Annual rainfall is between 650mm up to 2200 mm. Precipitation of next zone is between 400 to 200 mm yearly. The region 6 corresponds to South Zagros mountains. Its annual precipitation is between 260 to 150mm. Zone 7 is located in the northern margins of the desert (Dasht-e-Kavir). Zone 8 occupies the North-East of Iran, that is the zone with annual rainfall of 200 to 300 mm. The coastal region of Oman sea forms the zone 9. The zone number 10 comprises the Lut desert with very scarce precipitation over the whole year. The eleventh zone is located in the South-East of Iran and strongly influenced by monsoon (Table 1).

Table.1 Overall summary of geographical characters of precipitation zones of Iran

Precipitation Zones	Annual Precipitation(mm)	Geography Location
1	250–600	Aras Basin (NW of Iran)
2	280–850	Urmia Basin
3	250–1400	Zagros Mountain
4	650–2200	Caspian Sea coast
5	250–500	South slop Alborz mountain
6	150–300	Khuzestan plain-Bandar-Abaas
7	100–300	Central mountain and desert
8	100–250	North east (Khorasan)
9	100–200	North Oman Sea
10	30–100	Lut and Dasht Kavir
11	80–200	East of Iran

[3] - National Center for Environmental Prediction-National Center for Atmospheric Research NCEP/NCAR Reanalysis

3. Results And Discussion

Geographical analysis of Iran's rainfall shows that the spatial and temporal distribution of Iran's rainfall is significantly asymmetric. The annual rainfall of 30 mm in the Lut desert is up to 2,400 mm in the southwest of the Caspian Sea. The sequential wet and drought years in Iran are among other indicators of rainfall in this country (Table 2 & Fig. 2).

Table.2: Summary of features Annual Rainfall of Iran

Average(mm)	STDV	C.V %	Skew	Max(mm)	Min(mm)
241.1	53.4	21.5	0.3	377	138.20

The average annual rainfall in Iran is 248.1 mm with a variation coefficient of 21.5% and a range of 239 mm. In addition, positive skewness indicates that frequency of year with rainfall below the mean is more than the year with rainfall above the mean.

3.1. Linkage between Precipitation zones and 500 hPa level, SLP and SST (Repeated Patterns):

The relationships between the precipitation in Iran and large-scale atmospheric patterns were investigated based on correlation analysis. Initially, the repeating patterns of each map were determined. In the maps of the 500 hPa level, two distinct regions are found in almost all the bordering areas, one on the Baltic Sea, which is generally positively correlated with rainfall, and the other region located in different areas including the Red, Caspian, Black Sea, and parts of western Iran. The correlation of these regions with Iran's rainfall is negative (Fig. 3).

Figure 3 shows a repeated paradigm in all precipitation regions except zones 1 and 5. The second area (with the negative correlation) affects 7 zones. Whereas zones 9 and 11 are affected by region 1 (Baltic Sea).

In the SLP figures, the two regions that were specified included a region with a negative correlation with the Red Sea and the other with a positive correlation with the Indian Ocean, and in particular near Australia (Fig. 4). As mentioned before, the Red Sea and Indian Ocean regions are repeated throughout the precipitation regions. Six districts are affected by the first region (with negative correlation). The second area has been effective in five precipitation zones.

Recent researches show that the main sources of precipitation moisture in Iran are Caspian Sea, Persian Gulf, Arabian Sea, and Red Sea (Rousta et al., 2016; Ghaedi et al., 2012; Rahimi et al., 2010). Based on Fig. 5a region in the Arabian Sea has been repeated in all maps with a positive correlation, except first and second zones. The issue to be considered is that, although the impact of this region on providing Iran's precipitation humidity is clear, this study did not find any effect on the precipitation zones, only in fourth zone.

The correlation of these regions with the precipitation in Iran was determined by using multilinear regression and the best regression equation was defined. To achieve the best R^2, R^2 adjusted and P-value in the best regression equation, some areas, especially the SST, have been ignored (table3). As shown in Table 3 the regression equation for zones number 5,7, and 8 were not acceptable.

Table.3. The Regression Equation for 11 Anomaly of Precipitation regions of Iran

Precipitation Zones	Regression Equation	R^2	R^2_adj	R^{**}
1	AP* = -0.384–0.1499 (hgt2) − 2.164 (slp1) + 1.901 (slp2)	0.53	0.47	0.73
2	AP = -0.18–0.450 C2(hgt2) + 5.35 (slp2)	0.41	0.36	0.64
3	AP = -0.29–0.436 (hgt2) − 10.62 (slp1) + 10.21 (slp2)	0.51	0.45	0.71
4	AP = -0.47–0.2445 (hgt2) − 5.05 (slp1) + 17.84 (sst1)	0.70	0.67	0.84
5	No acceptable equation	-	-	-
6	AP = 0.28–0.876 (hgt2) − 15.45 (slp1) + 23.29 (slp2)	0.65	0.61	0.81
7	No acceptable equation	-	-	-
8	No acceptable equation	-	-	-
9	AP = 0.79 + 0.3069 (hgt1) - 13.30 (slp1) + 5.03 (slp2)	0.64	0.60	0.80
10	AP = -0.14–0.521 (hgt2) + 6.67 (slp2)	0.48	0.44	0.69
11	AP = 0.67 + 0.1796 (hgt1) − 0.287 (hgt2) − 8.14 (slp1)	0.53	0.48	0.73
*Anomaly of Precipitation ** Correlation value				

3.2. Relationship between Precipitation zones and 500 hPa level, SLP and SST:

Given that the regions repeated (regions where have physical justification for the linkage with the precipitation in Iran) could not play an effective role in the regression equations, more distant regions were also considered. Firstly, the simultaneous correlation between 11 precipitation zones of Iran and SLP, SST, and 500 hPa level were analyzed. The regions with correlation exceeding 0.3 are further tested for the regression equations. However, not all of them provide the high value of R^2 and P-value, so for the resulting regression equation we use the region that ensure the best statistical characteristics that marked on the Figs. 6 up to 8. After analyzing the correlation maps of all regions with a correlation of more than 0.3, correlation analysis and determination of regression equation was used. Of all the used areas, 12 regions that had the most impact on the regression equation of the precipitation regions of Iran were selected. It should be noted that sometimes a region had better correlation with Iran's precipitation, but it was neglected due to less effective role in the regression equations. these12 regions were determined as follows:

1-Baltic Sea/East of Europe, 2-Caspian Sea/Black Sea, 3-Mediterranean Sea, 4-Arabian Sea/ Red Sea/ Saudi Arabia/Iraq, 5-Africa/ Madagascar, 6-Australia/ Indian Ocean, 7- North Atlantic Ocean (west of Europe), 8-South Atlantic Ocean (East of south America), 9-North Pacific Ocean (west of North America), 10-South Pacific Ocean (South-East of Asia), 11-Greenland / Northwest of Europe, 12-East of Iran.

Figure 6 displays the simultaneous correlation between H500 and precipitation anomalies in 11 areas of Iran. The highest correlation between mid-tropospheric circulation and precipitation of Iran is associated to the following circulation patterns:

The higher pressure over north-east Atlantic and Northern Europe coupled with lower pressure over the Middle East (including the territory of Iran) is strongly correlated with increased precipitation in all regions. The mid tropospheric high to the north-west of Iran and trough located over the Middle East forms the current that counters the north-east periphery of 500 hPa anticyclone and that directs toward Iran bringing warm and humid air from the Atlantic. However, the pair of mid-tropospheric patterns provides the best regression only for zone 11, while the eastern-central part of Iran (regions 8 and 10) the geopotential in these patterns cannot be used as a good predictor of precipitation in spite of rather high correlation due to the small R^2 value. For other regions only mid tropospheric trough serves as a good predictor of precipitation amount.

Zone number 5 presents an exclusion with no influence of aforementioned coupled circulation patterns, but high positive correlation with the 500 hPa over the North Atlantic and low pressure over the subtropics. This may be interpreted as a smaller pressure gradient between Island depression and Azure high, accompanied by suppressed western current favors the higher precipitation on the windward slopes of Alborz mountains. The strong zonal current results in intensive water transport to northern and western Europe while longitudinal displacement of centers of action over the Atlantic causes the north-western current. This in turn guides the humid air from the Caspian Sea toward zone 5.

Analyzing the correlation figures we may distinguish several remote regions strongly correlated to the precipitation in Iran. However, the physical mechanism of these teleconnections is questionable. Therefore, it is not preferred to use the meteorological characteristics in such remote areas as predictors of Iran precipitation. Nevertheless, for some regions the excluding of these regions from the regression equation results in significant decrease of R^2 value. In this case we added these areas to the list of predictors. For region 2 geopotential at 500 hPa over South America is influential for precipitation. Noteworthy that this area is a part of the belt of negative correlation located in subtropics. Moreover, the distribution of correlation coefficient is consistent with the mean distribution of geopotential in the mid troposphere characterized by the zonal alternation of high- and low-pressure zones. The sign of correlation may be interpreted as follows: normal geopotential distribution with depressions over the equator and mid latitude and high pressure over the subtropics is correlated with decreased precipitation in Iran.

Previous studies have pointed out the role of Middle East circulation patterns at 500 hPa in precipitation of Iran (Lashkari, 2005; Ataei, 2009; Raziei et al.,2009; Alizade et al., 2013; Mohammadi, 2015). But our study emphasized the remote influence of mid tropospheric circulation over the Atlantic and Europe on the precipitation of Iran.

The analysis of sea level influence on the precipitation of Iran shows that winter rainfall is mostly related to the cyclonic activity with the center located to the south of Iran. The south-eastern current along the eastern periphery of the depression bring the moisture from the Persian Gulf and Indian ocean toward Iran. Note that for zone 1 located in the north of Iran the area of highest correlation is shifted to the north as compared to other precipitation regions. For zones 2 and 9 the area of high negative correlation is detected over the Middle East. However, inclusion of this region to the regression equation decreases the R^2.

Another correlation pattern appears over the equatorial Indian ocean. The positive correlation corresponds to the more abundant precipitation related to the higher pressure in this area. The pressure over the Indian ocean in winter determines the intensity of winter monsoons, the higher pressure over the ocean leads to weaker monsoons and less penetration of cold dry air from Siberia into Iran, which in turn results in more precipitation. However, SLP of Indian ocean does not always lead to improved regression results (zones 5,9,11).

The sea surface temperature has lower effect on the precipitation in Iran, than atmospheric circulation. Two main influential regions are the Mediterranean Sea and the region of coastal upwelling near Somali. The SST in the Mediterranean influences the precipitation in zone 5, while the high positive correlation near the African coast appears for almost all precipitation zones, but it is significant in regression equation for precipitation zones number4, 5 and 9. Possible mechanism involves intensity of upwelling and zonal wind. The lower SST associated with smaller precipitation (positive correlation) is a consequence of intensive upwelling near the coast. The latter results from more intensive westerly winds, that drive water off coast. Meanwhile, westerly wind anomalies are related to the stronger winter monsoon that transport cold and dry air from Siberia and yields to the reduction of precipitation amount.

Table 4

contains regression equations that are concluded from the combination of effective areas in 500 hPa, SLP and SST for each precipitation zones. This table shows the R^2 and R^2 adjusted for each zone. In the multiple linear regression models, the predictions may become biased due to the increase in predictors, which causes overfitting of the model. It is obvious that if the number of predictors increases, the accuracy of the model also increases. Each time a new predictor will be introduced, it may contribute to a better agreement of model with observed values, even if due to chance alone. Secondly, more predictors with higher ordered polynomials lead to the creation of random noises that produce high values of $R^{2,}$ which can be misleading. To combat such problems, the adjusted R^2 is considered, which becomes adjusted in accordance with the number of predictor variables. The value of the adjusted R^2 increases when a new predictor improves the model more than expected by chance and decreases if a predictor improves the model less than what is expected by chance (Swain et al,2017 Quoted from Yu et al,2015).

Table.4. The Best Regression Equation for 11 Anomaly of Precipitation regions of Iran

Precipitation Regions	Regression Equation	R^2	R^2-adj	R
1	AP*= -0.243–0.1761 (hgt2) - 1.532 (slp6) + 6.68 (sst10)	0.64	0.60	0.80
2	AP= -1.21–0.404 (hgt2) - 0.687 (hgt8) + 4.14 (slp6) + 7.02 (sst11)	0.69	0.64	0.83
3	AP = 0.81–0.342 (hgt4) - 9.74 (slp4) + 38.86 (sst7)	0.55	0.49	0.74
4	AP= -0.227 + 0.0884 (hgt1) - 2.315 (slp12) - 3.92 (slp8) + 16.24 (sst4)	0.81	0.78	0.90
5	AP = 0.076 + 0.0329 (hgt11) - 7.65 (slp4) - 4.81 (sst3) + 6.15 (sst10)	0.80	0.76	0.89
6	AP = -0.28–0.672 (hgt4) - 9.08 (slp7) + 43.2 (sst4)	0.66	0.62	0.82
7	AP= -0.100–0.1060 (hgt2) + 4.39 (slp8) + 7.98 (sst7)	0.55	0.50	0.74
8	AP = -0.04–0.1422 (hgt2) + 0.614 (hgt10) + 6.03 (slp6) - 5.35 (sst10) - 5.25 (sst10)	0.72	0.66	0.85
9	AP = 1.26 + 0.3608 (hgt1) - 0.350 (hgt6) + 0.2376 (hgt10) - 7.66 (slp4) - 9.31 (slp7)-15.97 (sst10)	0.91	0.88	0.95
10	AP= -0.19–0.367 (hgt9) - 4.79 (slp7) - 1.385 (slp11) + 15.00 (sst4) + 8.61 (sst5)	0.81	0.76	0.90
11	AP = 1.21 + 0.2368 (hgt1) - 9.68 (slp7) - 17.41 (sst10)	0.72	0.68	0.85

According to the calculations, based on regression equation anomaly of each precipitation zones were calculated. Correlation between observed data and calculated data are shown in Fig. 10. The high correlation between the calculated data with the regression equations and the observed data is evident.

4. Conclusion

Changes in winter precipitation in Iran have caused positive anomalies (heavy rainfall) and negative anomalies (droughts) in Iran. Changes in sea surface temperature, sea level pressure,500 hPa and blocking systems are effective on winter precipitation anomalies in Iran. In fact, the atmosphere-ocean interaction at the Earth's surface plays an important role in the occurrence of precipitation anomalies in Iran.

The results indicated that decreased pressure on the Red Sea (Sudan Low) and the Pacific Ocean and increased pressure on the Atlantic and Indian oceans increase Iran's winter precipitation. In 500hpa, the results indicated that increased winter precipitation in Iran is associated with an increase in altitude of 500hPa on the Baltic Sea and the Indian Ocean and a decrease in altitude of 500hPa on the Caspian Sea, the Mediterranean Sea, the Arabian Sea and the Red Sea. In SST, the results indicated that the linkage between SST and precipitation of Iran is positive in regions such as the Arabian and Red sea, Madagascar, and north Atlantic Ocean. Negative correlation can be seen with Mediterranean Sea and south Pacific Ocean. Therefore, any change in sea level pressure, 500hPa level and sea surface temperature leads to positive and negative anomalies on Iran's rainfall. Therefore, global warming, which leads to changes in SLP, atmospheric thickness (1000 – 500) and SST, has a greater impact on Iran's rainfall and leads to challenges in water resources and climate risks.

References

1. Ahmadi, M., Salimi, S., Hosseini, S. A., Poorantiyosh, H., & Bayat, A., 2019. Iran's precipitation analysis using synoptic modeling of major teleconnection forces(MTF). Dynamics of Atmospheres and Oceans, Vol.85.,41-56.
2. Alijani, B., 2008. Effect of the Zagros Mountains on the spatial distribution of precipitation. Journal of Mountain Science, 5(3), 218-231.
3. Alizade, T., Azizi, G., Rousta, I., 2013. Analysis of 500 hPa circulation patterns of the event pervasive and non-pervasive precipitation in Iran, The Journal of Spatial Planning, Vol.16, No,4:1-24.
4. Ataei, H., 2009, 500 hpa Map Patterns Associated with Low Precipitation Years in Iran, Geography and Environmental Planning,33(1):43-58. (In Persian).
5. Azmoodehfar, M. H., Azarmsa, S. A., 2013. Assessment the effect of ENSO on weather temperature changes using fuzzy analysis (case study: Chabahar). APCBEE procedia, 5, 508-513.
6. Barandiaran, D., Wang, S. Y., 2014. The missing teleconnection between the North Atlantic and the Sahel precipitation in CFSv2. Atmospheric Science Letters, 15(1), 21-28.
7. Barnston, A. G., Livezey R.E., 1987. Classification, seasonality and persistence of low-frequency atmospheric circulation patterns. Monthly weather review, 115(6), 1083-1126.
8. Barth, H.J. and Steinkohl, F., 2004. Origin of Winter Precipitation in the Central Coastal Lowlands of Saudi Arabia. Journal of Arid Environments 52: 101-115.
9. Brown, D. P., Comrie, A. C., 2002. Sub-regional seasonal precipitation linkages to SOI and PDO in the Southwest United States. Atmospheric Science Letters, 3(2-4), 94-102.

10. Darand, M., Daneshvar, M. R. M., 2014. Regionalization of precipitation regimes in Iran using principal component analysis and hierarchical clustering analysis. Environmental Processes, 1(4), 517-532.
11. Davey, M. K., Brookshaw, A., Ineson, S., 2014. The probability of the impact of ENSO on precipitation and near-surface temperature. Climate Risk Management, 1, 5-24.
12. Delju, A. H., Ceylan, A., Piguet, E., & Rebetez, M., 2013. Observed climate variability and change in Urmia Lake Basin, Iran. Theoretical and applied climatology, 111(1-2), 285-296.
13. Dezfuli, A. K., Karamouz, M., Araghinejad, S., 2010. On the relationship of regional meteorological drought with SOI and NAO over southwest Iran. Theoretical and applied climatology, 100(1-2), 57-66.
14. Doostan, R., Alijani, B., 2016. Climate change of Iran: A synoptic approach. Journal of Geography and Regional Development, 13(25), 89-113.
15. Farajzadeh, M., Ahmadi, M., Alijani, B., Qavidel Rahim, Y., Mofidi, A., Babaeian, I., 2014. Study on Variation of Major Teleconnection Patterns (MTP) associated with Iran's Precipitation, Climatology Research, No.15:31-45 (In Persian).
16. Farajzadeh, M., Khorany, A and Lashkary, H (2008), The Relation Between Jet Stream Location and Cyclones Over the Western Iran, American Journal of Applied Sciences 5 (10): 1308-1312.
17. Fatemi, M., Omidvar, K., Beiglou, K. H. B., & Narangifard, M., 2015. Using principle component analysis in identifying synoptic patterns of wet periods in Central Iran. J Earth Sci Clim Change, 6(309), 2.
18. Ghaedi, S., Movahedi, S., Masoodian, A., 2012. The Relation between the Red sea trough and heavy precipitation in Iran, Geography and environment sustainability, Vol 1, No 2, 1:8 (In Persian).
19. Ghasemi, A., Khalili, D., 2008. The association between regional and global atmospheric patterns and winter precipitation in Iran, Atmospheric Research, Vol. 88, Issue 2:116-133.
20. Goharnejad, H., Shamsai, A., Hosseini, S.A., 2013. Vulnerability assessment of southern coastal areas of Iran to sea level rise: evaluation of climate change impact, Oceanologia 55(3):617-637.
21. Gushchina, D., Dewitte, B., 2011. The relationship between intra seasonal tropical variability and ENSO and its modulation at seasonal to decadal timescales. Central European Journal of Geosciences, 3(2), 175-196.
22. Hauke, J., & Kossowski, T., 2011. Comparison of values of Pearson's and Spearman's correlation coefficients on the same sets of data. Quaestiones geographicae, 30(2), 87-93.
23. Javari, M., 2016. Trend and Homogeneity Analysis of Precipitation in Iran, Climate, 4, 44:1-23.
24. Kalnay E., Kanamitsu, M., Kistler, R., Collins, W., Deaven, D., Gandin, L., Iredell, M., Saha, S., et al., 1996. The NCEP/NCAR 40-Year Reanalysis Project. Buli. Amer. Meteor. Soc, 1996, 77, 437-471
25. Lashkari, H., 2005. Synoptic analysis of two samples of winter rainfall pattern in the South East of Iran, Modarres Human science, Vol,9, No.1:169-196 (In Persian).
26. Leathers, D.J., 1988. The Pacific/North American Teleconnection Index and United State Climate, A PhD Thesis in Geography, The Pennsylvania State University, Department of Geography.

27. Lee, J. H., Julien, P. Y., 2016. Teleconnections of the ENSO and South Korean precipitation patterns. Journal of Hydrology, 534, 237-250.
28. Lichtenstern, A., 2013. Kriging methods in spatial statistics, Bachelor's Thesis, Supervisor: Prof. Dr. Claudia Czado, Technische Universit¨at Mu¨nchen, Department of Mathematics.
29. Lu, M., Lall, U., Kawale, J., Liess, S., & Kumar, V., 2016. Exploring the predictability of 30-day extreme precipitation occurrence using a global SST–SLP correlation network. Journal of Climate, 29(3), 1013-1029.
30. Meidani, E., & Araghinejad, S., 2014. Long-lead streamflow forecasting in the southwest of Iran by sea surface temperature of the Mediterranean Sea. Journal of Hydrologic Engineering, 19(8), 05014005.
31. Mohammadi, B., 2015. Locating the 500 hPa Squares Effect on Iran's Climate in the Cold Weather of the Year, Geographical research, Vol 29, No.4:113-132 (In Persian).
32. Motamedi, M., Ehteramian K., Shahab far A.R., 2007. The Study of Teleconnection Between ENSO as a Weather Signals and Rain Fall and Temperature Fluctuations of the Khorasan Province, Environmental Sciences, Vol.4(4). 75-90.
33. Nazemosadat, M. J. & Ghasemi, A. R., 2004. Quantifying the ENSO Related Shifts in the intensity and probability of drought and wet periods in Iran. *J. Climate*., *17* (20), 4005-4018.
34. Nazemosadat, M. J., Samani, N., Barry, D. A., Molaii Niko, M., 2006. ENSO forcing on climate change in Iran: precipitation analysis. Iranian Journal of Science and Technology, Transaction B: Engineering, 30, 555-565.
35. Obilor, E. I., & Amadi, E. C., 2018. Test for Significance of Pearson's Correlation Coefficient. International Journal of Innovative Mathematics, Statistics & Energy Policies, 6(1), 11-23.
36. Ptak, M., Tomczyk, A. M., Wrzesiński, D., 2018. Effect of teleconnection patterns on changes in water temperature in Polish lakes. Atmosphere, 9(2), 66.
37. Rahimi, D., Khoshhal, J., Alizade, T., 2010. The statistic-synoptic analysis of heavy showers in arid regions of Iran: Kerman province, Journal of geography and regional development, No 14, 51:69 (In Persian).
38. Rasouli, A. A., Babaeian, I., Ghaemi, H., & ZawarReza, P.,2012. Time series analysis of the pressure of the synoptic pattern centers affecting on seasonal precipitation of Iran. Geography and Development, No.27,18-21.
39. Raziei, T., Bordi, I., Santos, J. A., Mofidi, A., 2013. Atmospheric circulation types and winter daily precipitation in Iran. International Journal of Climatology, 33(9), 2232-2246.
40. Raziei, T., Mofidi, A., Zarrin, A., 2009, The 500 hPa atmospheric centers of action and circulation patterns over the Middle East and their relationship with precipitation in Iran, Journal of the Earth and Space Physics. Vol,35, No,2:121-141 (In Persian).
41. Rezaebanafsheh, M., Jahanbakhsh, S., Bayati, M., & Zeynali, B., 2011. Forecasting autumn and winter precipitation of west of Iran applying Mediterranean SSTs in summer and autumn. Physical Geography Res Q, 74(4), 47-62.

42. Rousta, I., Soltani, M., Zhou, W., Cheung, H.H., 2016. Analysis of extreme precipitation events over central plateau of Iran. Am. J. Clim. Chang., 5, 297.
43. Roy, S. S., 2006. The impacts of ENSO, PDO, and local SSTs on winter precipitation in India. Physical Geography, 27(5): 464-474.
44. Sabziparvar, A. A., Movahedi, S., Asakereh, H., Maryanaji, Z., & Masoodian, S. A.,2015. Geographical factors affecting variability of precipitation regime in Iran. Theoretical and Applied Climatology, 120(1-2), 367-376.
45. Saji, N. H., Ambrizzi, T., Ferraz, S. E. T., 2005. Indian Ocean Dipole mode events and austral surface air temperature anomalies. Dynamics of atmospheres and oceans, 39(1-2), 87-101.
46. Schneider, U., Fuchs, T., Meyer-Christoffer, A., Rudolf, B., 2008. Global precipitation analysis products of the GPCC. Global Precipitation Climatology Centre (GPCC), DWD, Internet Publikation, 112.
47. Schober, P., Boer, C., & Schwarte, L. A., 2018. Correlation coefficients: appropriate use and interpretation. Anesthesia & Analgesia, 126(5), 1763-1768.
48. Swain, S., Patel, P., Nandi, S., 2017.A multiple linear regression model for precipitation forecasting over Cuttack district, Odisha, India. In Convergence in Technology (I2CT), 2017 2nd International Conference for (pp. 355-357). IEEE.
49. Trenberth, K. E., & Shea, D.J., 2005. Relationships between precipitation and surface temperature. Geophysical Research Letters, 32(14).
50. Türkes, M., Sümer, U. M., & Kiliç, G., 2002. Persistence and periodicity in the precipitation series of Turkey and associations with 500 hPa geopotential heights. Climate Research, 21(1), 59-81.
51. Uyanik, G. K., & Güler, N., 2013. A study on multiple linear regression analysis. Procedia-Social and Behavioral Sciences, 106, 234-240.
52. van der Ent, R. J., & Savenije, H. H., 2013. Oceanic sources of continental precipitation and the correlation with sea surface temperature. Water Resources Research, 49(7), 3993-4004.
53. Wallace, J. M., Gutzler, D.S., 1981. Teleconnections in the geopotential height field during the Northern Hemisphere winter. Monthly Weather Review, 109(4), 784-812.
54. Wibig, J., 1999. Precipitation in Europe in relation to circulation patterns at the 500 hPa level. International Journal of Climatology: A Journal of the Royal Meteorological Society, 19(3), 253-269.
55. Xoplaki, E., Luterbacher, J., Burkard, R., Patrikas, I., & Maheras, P., 2000. Connection between the large-scale 500 hPa geopotential height fields and precipitation over Greece during wintertime. Climate research, 14(2), 129-146.

Figures

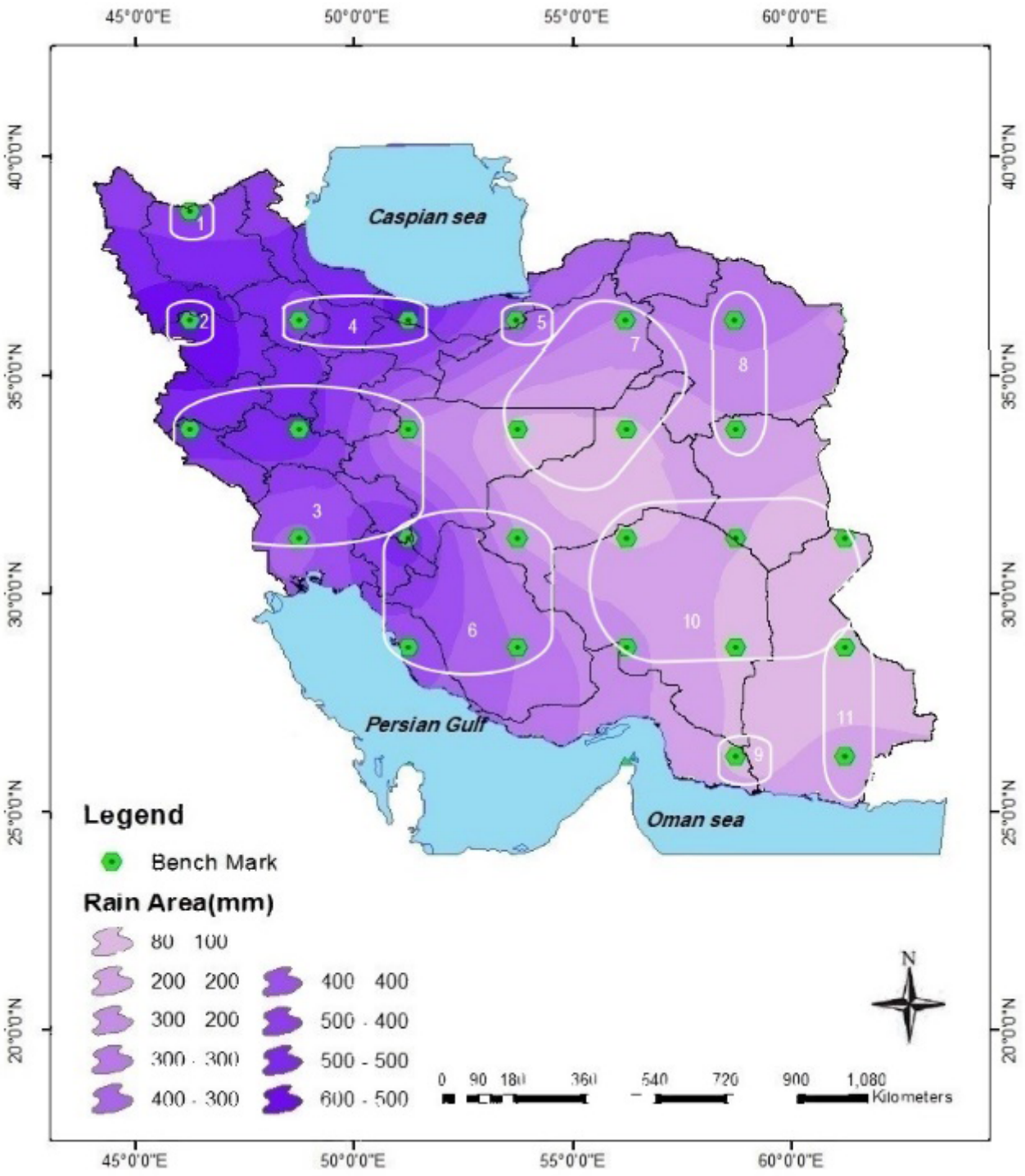

Figure 1

Precipitation (mm) zones over Iran using Kriging method (Green points =grid pixels; white frames= precipitation zones)

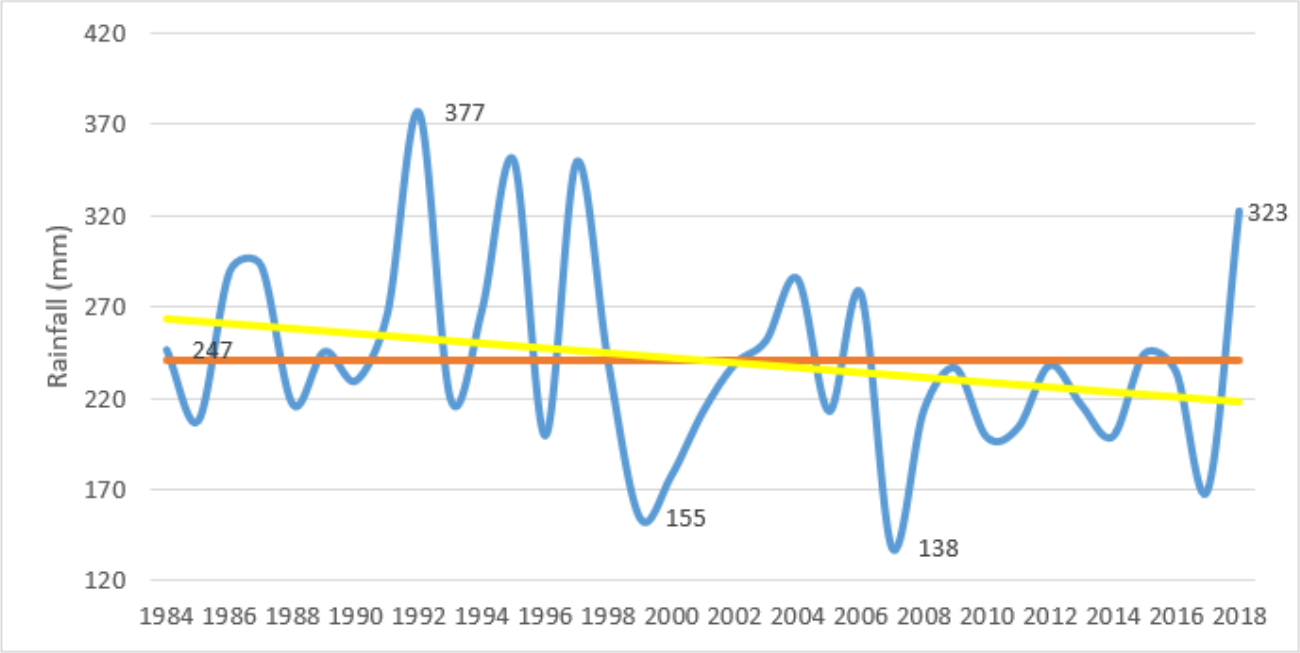

Figure 2

Iran's annual rainfall trend in period 1984-2018

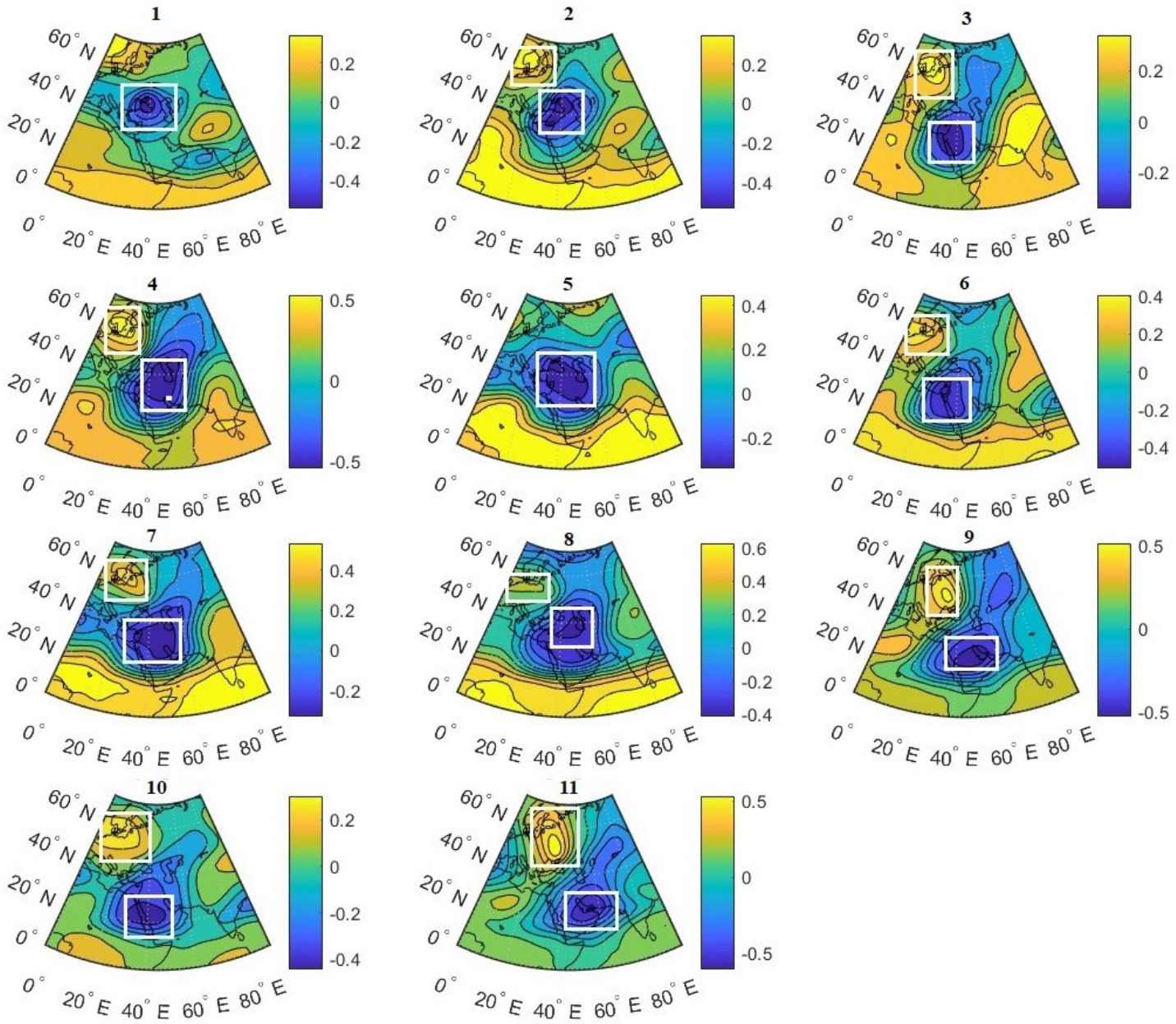

Figure 3

Linkage between 500 hPa and Precipitation zones of Iran (Regions with best correlation specified with white frame)

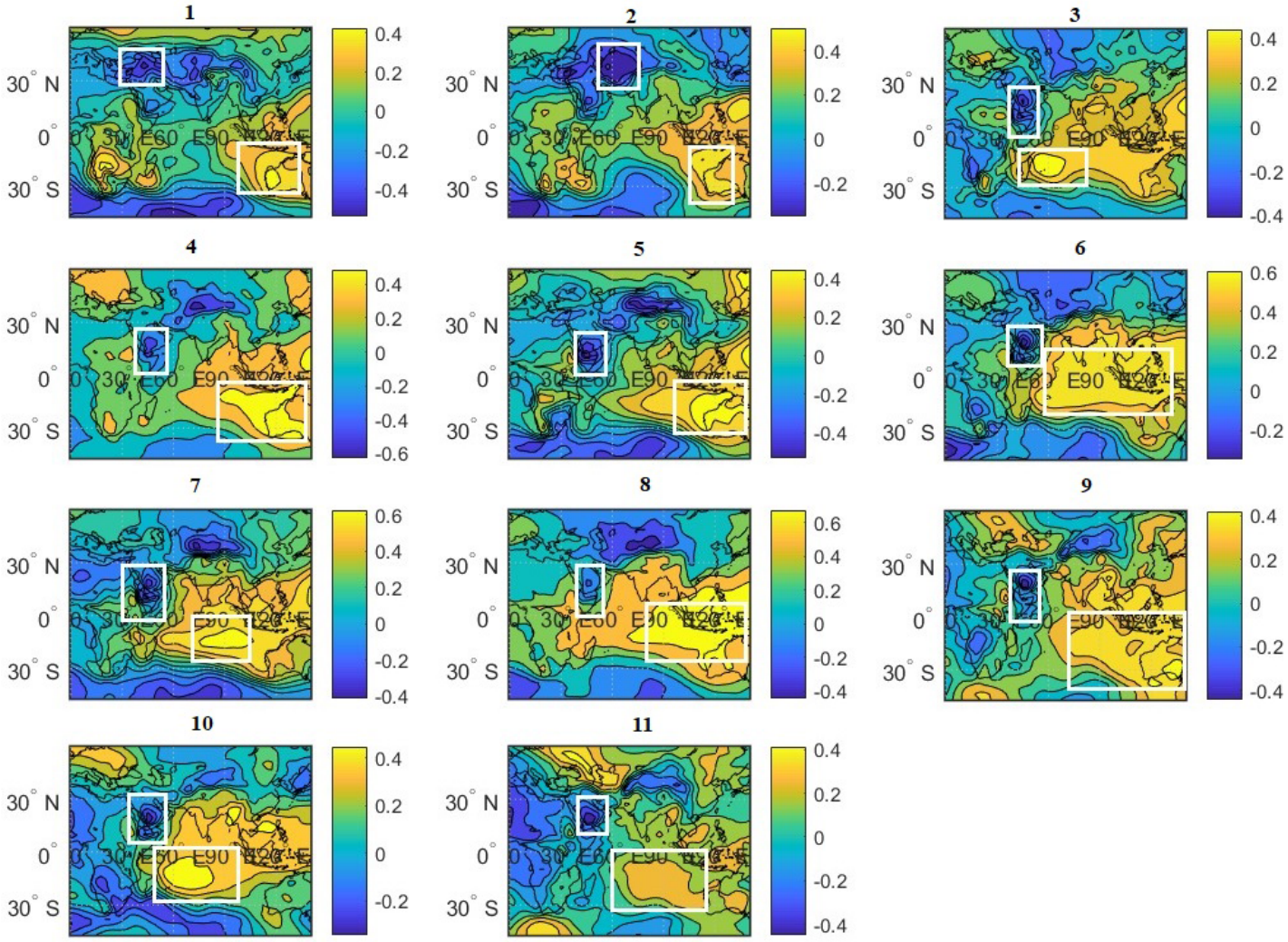

Figure 4

Linkage between SLP and Precipitation zones of Iran (Regions with best correlation specified with white frame)

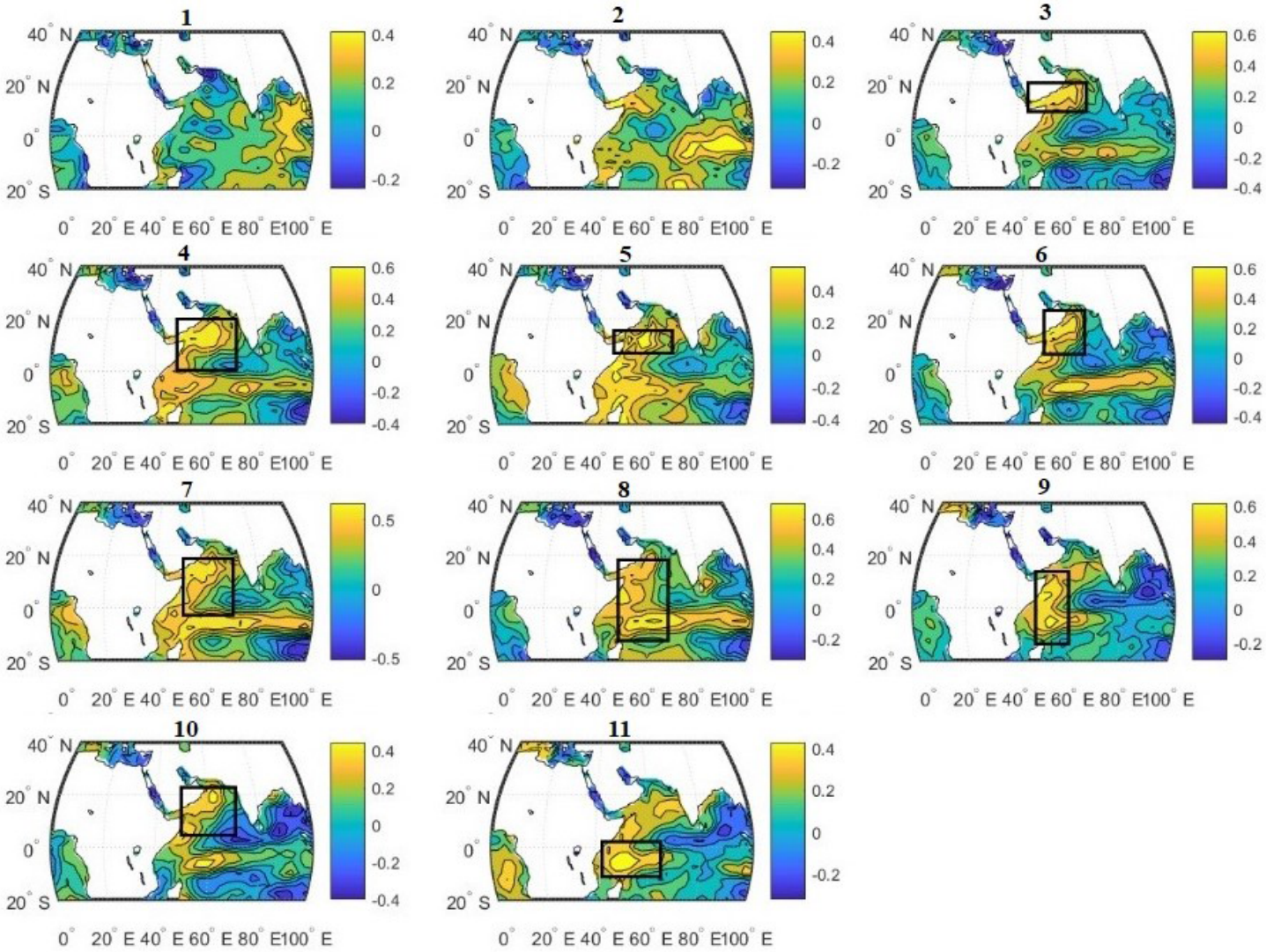

Figure 5

Linkage between SST and Precipitation zones of Iran (Regions with best correlation specified with black frame)

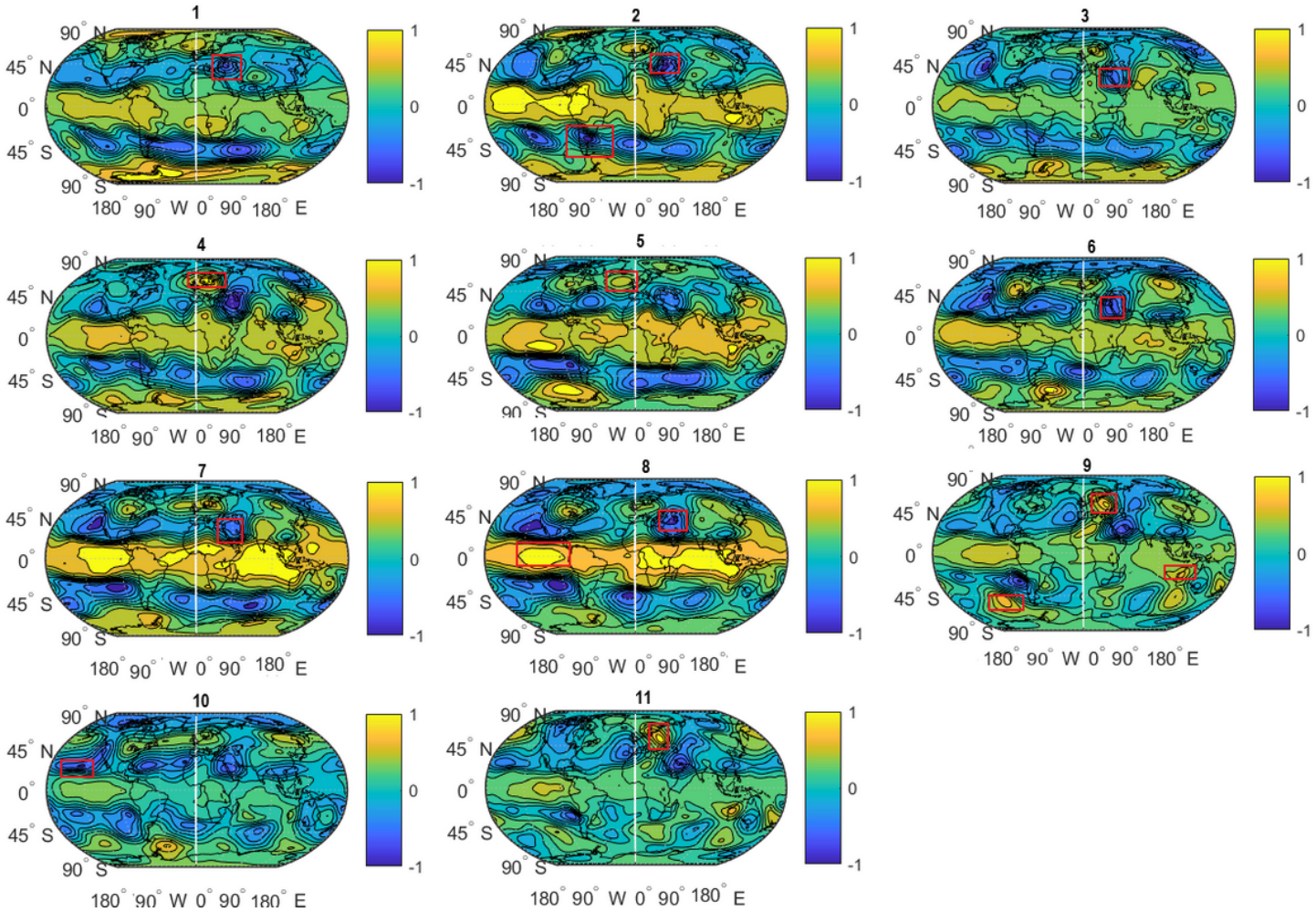

Figure 6

Correlation between 500 hPa level and winter precipitation of Iran (Regions with best correlation specified with red frame)

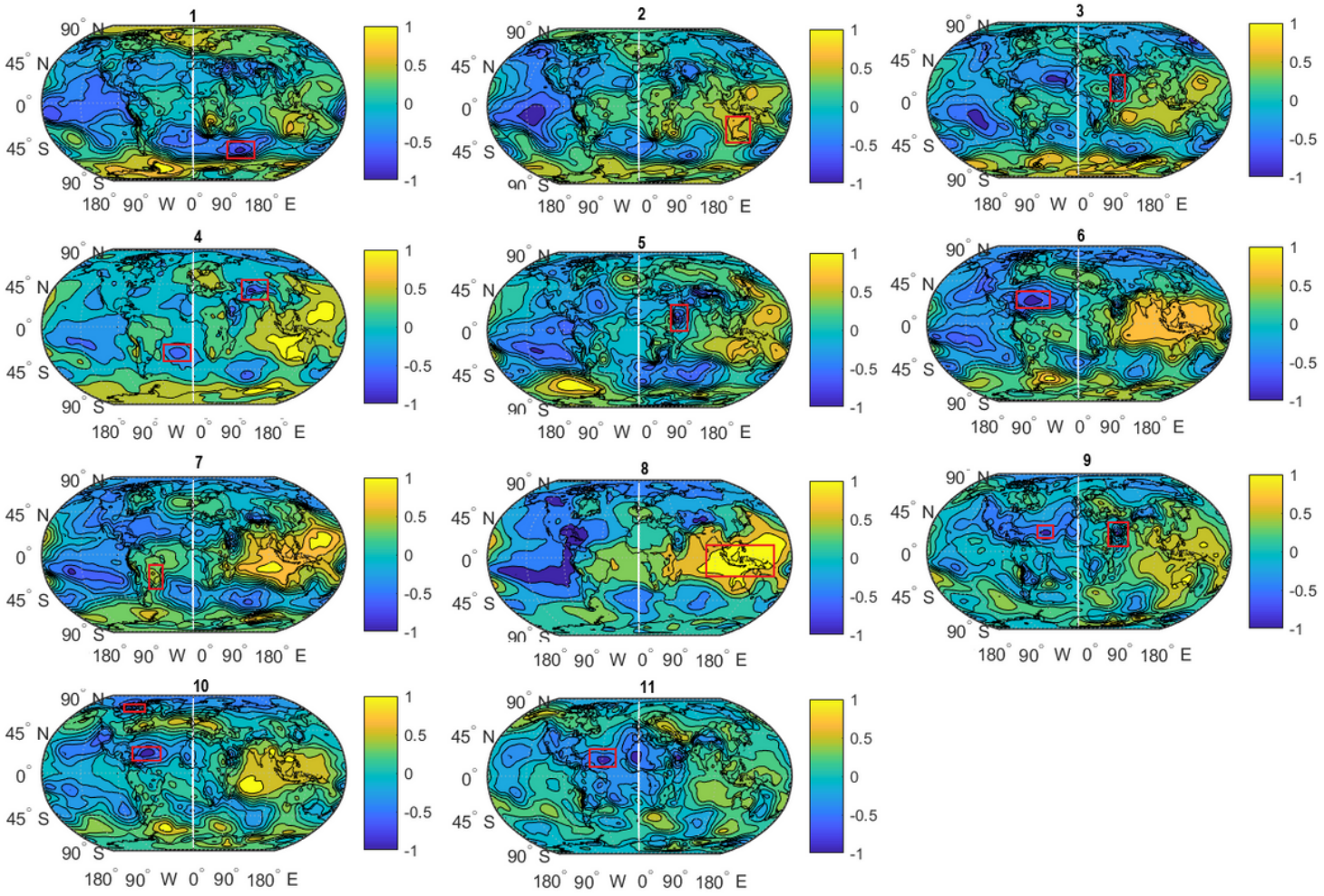

Figure 7

Correlation between SLP and winter precipitation of Iran (Regions with best correlation specified with red frame)

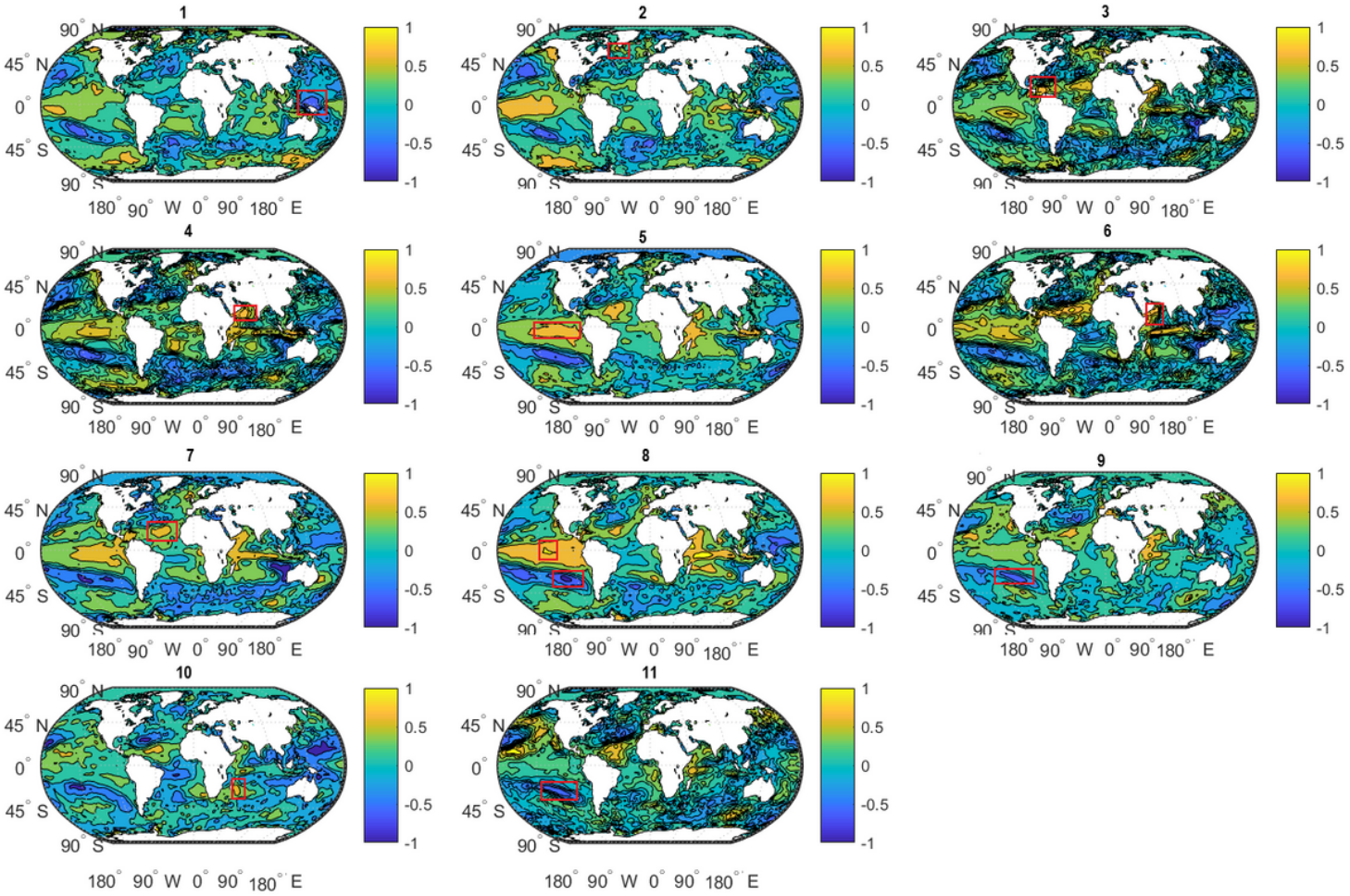

Figure 8

Correlation between SST and winter precipitation of Iran (Regions with best correlation specified with red frame)

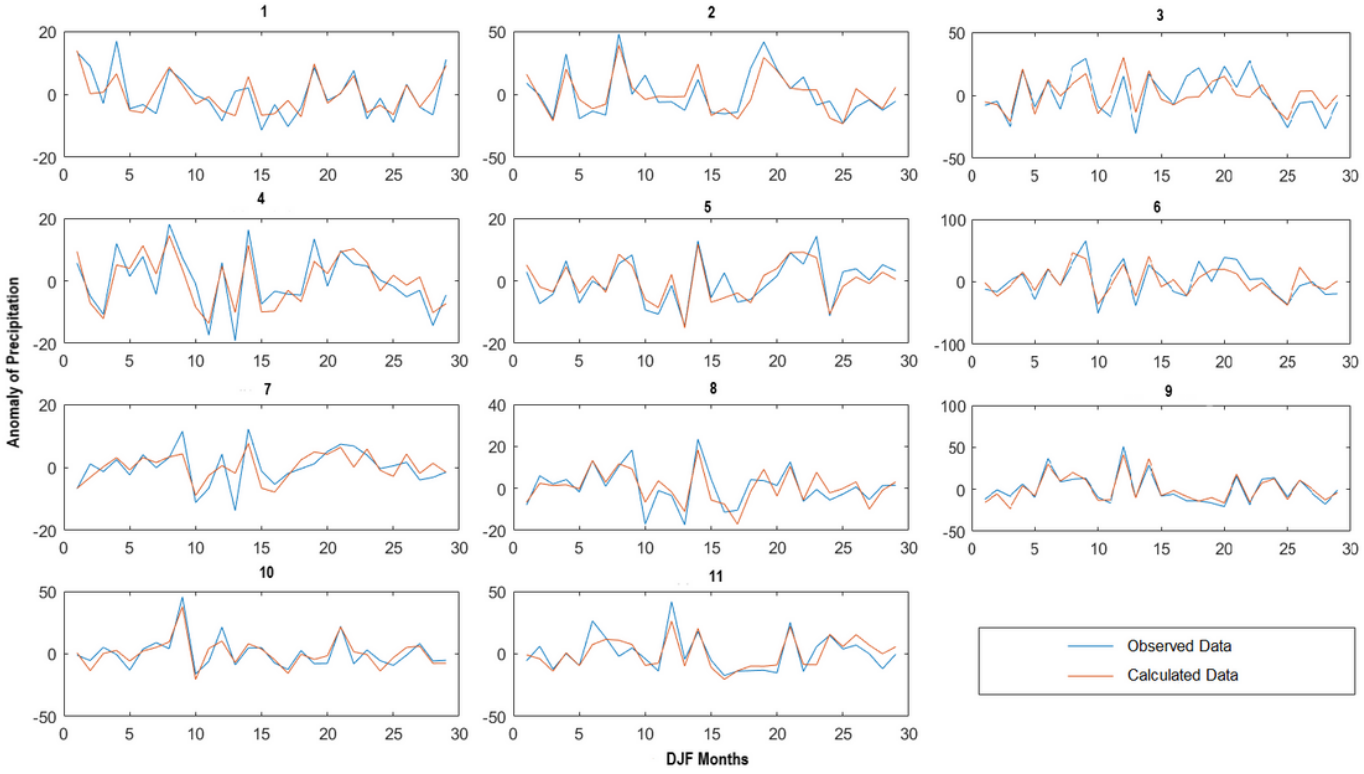

Figure 9

Fig.10. Plot of correlation between observed data and calculated data in precipitation zones